ELSEVIER

Journal of Biomechanics 40 (2007) 595–602

JOURNAL OF BIOMECHANICS

www.elsevier.com/locate/jbiomech
www.JBiomech.com

Prediction of the hip joint centre in adults, children, and patients with cerebral palsy based on magnetic resonance imaging

M.E. Harrington[a], A.B. Zavatsky[b,*], S.E.M. Lawson[b], Z. Yuan[b], T.N. Theologis[a]

[a]*The Oxford Gait Laboratory, Nuffield Orthopaedic Centre, Oxford, UK*
[b]*Department of Engineering Science, University of Oxford, Parks Road, Oxford OX1 3PJ, UK*

Accepted 1 February 2006

Abstract

The location of the hip joint centre (HJC) is required for calculations of hip moments, the location and orientation of the femur, and muscle lengths and lever arms. In clinical gait analysis, the HJC is normally estimated using regression equations based on normative data obtained from adult populations. There is limited relevant anthropometric data available for children, despite the fact that clinical gait analysis is predominantly used for the assessment of children with cerebral palsy. In this study, pelvic MRI scans were taken of eight adults (ages 23–40), 14 healthy children (ages 5–13) and 10 children with spastic diplegic cerebral palsy (ages 6–13). Relevant anatomical landmarks were located in the scans, and the HJC location in pelvic coordinates was found by fitting a sphere to points identified on the femoral head. The predictions of three common regression equations for HJC location were compared to those found directly from MRI. Maximum absolute errors of 31 mm were found in adults, 26 mm in children, and 31 mm in the cerebral palsy group. Results from regression analysis and leave-one-out cross-validation techniques on the MRI data suggested that the best predictors of HJC location were: pelvic depth for the antero-posterior direction; pelvic width and leg length for the supero-inferior direction; and pelvic depth and pelvic width for the medio-lateral direction. For single-variable regression, the exclusion of leg length and pelvic depth from the latter two regression equations is proposed. Regression equations could be generalised across adults, children and the cerebral palsy group.

Keywords: Gait; Hip joint centre; Motion analysis; MRI; Cerebral palsy

1. Introduction

In gait analysis, the hip joint centre (HJC) is the point about which hip moments are calculated, and it is often used in determining the location and orientation of the femur and in estimating the lengths and lever arms of muscles crossing the hip. Unlike prominent bony landmarks, such as the superior iliac spines, the HJC cannot be palpated and thus its location must be calculated. Errors in the location of the HJC can propagate down the limbs through kinematic and kinetic calculations.

Although clinical gait analysis is predominantly used for the assessment of children with cerebral palsy, the most common ways of estimating HJC rely on equations derived from average adult anthropometric data. These may not be appropriate for children, whose pelvic geometry is still maturing, and even less so for children with cerebral palsy who, almost invariably, have musculoskeletal deformities.

Previous studies found the error in HJC estimation in adults using a range of methods in living subjects (Kirkwood et al., 1999; Leardini et al., 1999) and cadaveric specimens (Seidel et al., 1995). Functional techniques, such as those proposed by Cappozzo (1984),

*Corresponding author. Tel.: +44 1865 273146; fax: +44 1865 273010.
E-mail address: amy.zavatsky@eng.ox.ac.uk (A.B. Zavatsky).

0021-9290/$ - see front matter © 2006 Elsevier Ltd. All rights reserved.
doi:10.1016/j.jbiomech.2006.02.003

calculate the HJC in a pelvis reference frame as the centre of the best-fit sphere described by the trajectories of markers placed on the thigh. Despite work suggesting that these techniques may be accurate even when applied to restricted ranges of motion (Piazza et al., 2001), they have been limited in their application to clinical settings. As a consequence, most clinical gait analyses still rely on prediction methods for determining HJC locations. Furthermore there is very little information available on HJC location in children or patients with musculoskeletal deformity (Fieser et al., 2000) and the implications of using regression equations based on adult data are not fully appreciated.

The present work uses magnetic resonance imaging (MRI) to assess three popular prediction techniques for the HJC and to quantify the errors involved in their application to healthy adults and children and to patients with cerebral palsy. New regression equations based on the MRI data are proposed.

2. Methods

Eight adults, 14 healthy children, and 10 children with spastic diplegic cerebral palsy (Table 1) gave informed consent and participated in this study, which was approved by the local ethics committee. MRI scans were taken of the pelvis using a 2.5 mm slice width T1-weighted, three-dimensional sequence to optimise bone and muscle definition, with a gradient echo (TE/TR 20/15 ms) to maximise the speed of acquisition. A two-dimensional volume spin-echo sequence was also collected to aid orientation within the former images. The leg lengths of each subject were measured manually from each anterior superior iliac spine to the ipsi-lateral medial malleolus, via the medial femoral epicondyle.

Medical imaging software (Analyze 5.0, Biomedical Imaging Resource, MN, USA) was used to locate the coordinates of the anterior and posterior superior iliac spines (ASIS, PSIS) within the scans. These coordinates

Table 1
Subject details with pelvic width (PW), pelvic depth (PD) and averaged hip joint centre (HJC) location derived from MRI images and leg length (LL) measured manually

Subject	Sex	Age	Mass	PW	PD	Leg length	Hip joint centre		
		(yrs)	(kg)	(mm)	(mm)	(mm)	*x*	*y*	*z*
H1	M	5.9	20.0	158.9	89.1	535	−24.5	−47.9	58.5
H2	M	6.0	21.5	171.2	96.2	602.5	−23.7	−58.3	60.1
H3	M	6.0	15.5	140.6	81.0	500	−26.1	−53.1	52.2
H4	F	6.1	21.5	156.2	97.3	612.5	−31.9	−60.6	60.0
H5	F	6.4	23.0	162.5	100.7	610	−28.0	−69.5	59.2
H6	F	8.1	22.5	171.8	93.7	695.5	−23.7	−65.4	62.8
H7	M	8.3	32.0	203.2	95.0	750	−34.6	−66.5	66.0
H8	F	8.5	27.5	181.5	106.3	687.5	−43.3	−64.0	61.8
H9	F	9.6	30.0	189.1	109.7	795.5	−33.9	−72.7	63.7
H10	M	9.8	34.5	173.4	110.2	785	−41.2	−69.3	64.5
H11	F	10.1	34.0	171.0	113.5	730	−37.9	−68.5	60.8
H12	M	11.4	36.5	213.2	103.8	780.5	−40.6	−78.1	75.9
H13	F	12.3	47.0	215.0	125.0	847.5	−48.7	−75.6	78.6
H14	M	13.0	44.0	228.2	121.3	880	−36.4	−79.7	72.4
A1	F	22.9	54.0	205.5	138.9	810	−41.4	−73.9	85.6
A2	M	24.1	79.0	275.6	163.2	980	−48.1	−91.8	96.1
A3	M	26.1	72.5	246.1	155.8	955	−43.6	−81.9	88.9
A4	F	27.0	69.0	231.5	152.5	920	−39.6	−86.6	94.6
A5	M	28.1	75.0	238.6	152.7	950	−49.7	−90.4	90.1
A6	F	32.6	56.0	238.4	142.5	865	−51.1	−88.2	86.1
A7	M	33.7	76.5	249.4	145.5	985	−33.4	−82.3	91.9
A8	M	40.1	81.0	276.1	164.2	950	−51.8	−95.2	95.7
C1	M	6.1	20.5	156.8	92.9	580	−37.2	−53.5	61.5
C2	M	8.0	20.0	149.9	91.7	580	−32.8	−57.4	57.2
C3	F	8.2	25.0	157.2	98.9	660	−37.1	−56.7	62.9
C4	F	8.3	22.5	180.1	83.1	630	−28.2	−59.9	60.9
C5	F	9.1	35.0	187.4	98.0	715	−22.9	−70.9	63.7
C6	F	10.6	30.0	160.0	102.5	700	−46.0	−65.2	68.0
C7	M	11.4	40.0	175.3	111.5	745	−40.3	−63.1	66.8
C8	F	11.5	27.0	182.1	106.1	730	−43.1	−64.6	73.4
C9	M	12.4	40.0	182.2	112.0	770	−33.7	−66.4	65.6
C10	M	12.5	29.5	188.0	90.6	700	−34.5	−67.5	70.1

H = healthy child, A = adult, C = child with spastic diplegic cerebral palsy. Body mass is given to the nearest 0.5 kg. Leg length is given as the average of left and right leg lengths, each measured to the nearest mm. Coordinates are given for a right HJC.

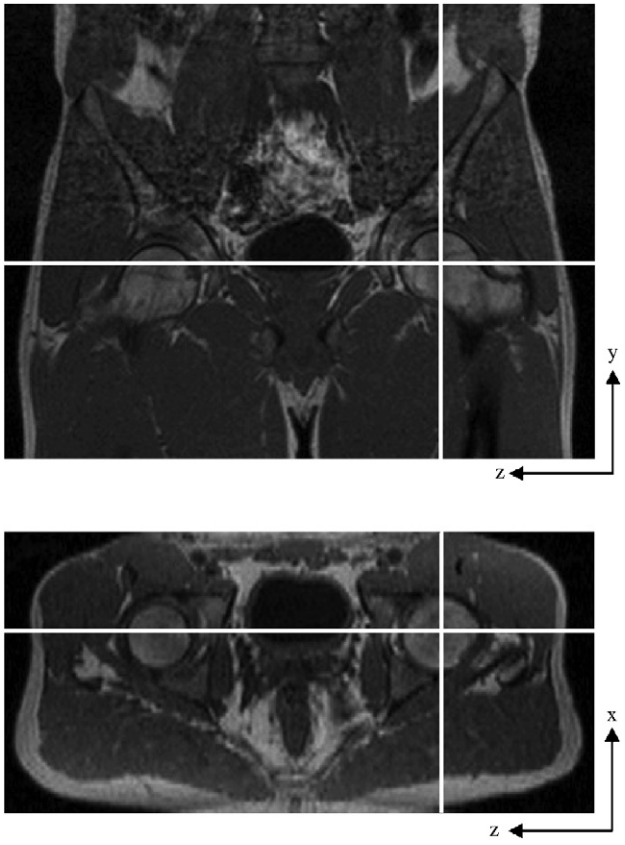

Fig. 1. Example coronal (top) and transverse MRI images through a pelvis showing a first approximation to the HJC location and the orientation of the pelvic coordinate system: z-axis passing through the ASISs from left to right, y-axis perpendicular to the plane containing the x-axis and the mid point of the PSISs and pointing superiorly, x-axis perpendicular to the yz plane, pointing anteriorly. Note that the coordinate system origin is located halfway between the two ASISs (Wu, 2002).

were used to define a pelvis-embedded coordinate system, with axis directions in accordance with International Society of Biomechanics guidelines (Wu, 2002) (Fig. 1).

The locations of both left and right HJCs were found using the MR images and an optimisation procedure. The medical imaging software was used to extract the 3D coordinates of a minimum of 30 points distributed over the surface of the femoral head (Fig. 1). It was assumed that the femoral head could be represented by a sphere of radius R with centre (x_c, y_c, z_c). A sphere was fitted by minimising the sum of squares of the distances from each data point to the surface of the sphere (Matlab Optimization Toolbox; Mathworks, Inc., Natick, MA, USA). Initial values for (x_c, y_c, z_c) in the optimisation came from a visual estimate of the HJC in the MRI scans (Fig. 1); the initial value of R was taken to be the average distance of all the selected points from this estimated HJC. For each subject, the coordinates of the left and right HJCs were compared to give an estimate of pelvic asymmetry.

Table 2
Prediction equations from the literature for the right hip joint centre (HJC) coordinates in the pelvis

	Method I	Method II	Method III
HJCx	$-0.95X\text{dis}+0.031\text{LL}-4$	-0.19PW	-0.22PW
HJCy	$-0.31X\text{dis}-0.096\text{LL}+13$	-0.30PW	-0.34PW
HJCz	$0.5\text{PW}-0.055\text{LL}+7$	0.36PW	0.32PW

PW = pelvic width (mm), LL = leg length (mm). $X\text{dis}$ = anterior/posterior component of the distance (mm) from the ASIS to HJC in the sagittal plane that can be measured from a clinical examination or more usually estimated from the regression equation $X\text{dis} = 0.1288(\text{LL}) - 48.56$ (Vicon Clinical Manager user manual, Oxford Metrics Ltd., 1995).

The MRI scans of four subjects (one adult, two children, and one child with cerebral palsy) were used to quantify the intra- and inter-assessor error in identifying the coordinates of the anatomical landmarks, the resulting orientations of the pelvic coordinate axes, and the final location of the HJCs. One researcher extracted data from each of the scans on four consecutive days. A second researcher followed the same protocol, but extracted data from each scan only once. Only one HJC per subject was analysed.

The averaged coordinates of the left and right HJCs (x, y, z) for each subject from the MRI scans were compared to those calculated using three predictive methods with widespread use in clinical gait analysis (Table 2). Method I (Davis et al., 1991) was implemented using leg length (LL, measured manually) and pelvic width (PW, the inter-ASIS distance from the MRI scans). Method II (Bell et al., 1990) and Method III (software recommendations for OrthoTrak, Motion Analysis Corp., CA, USA) relied on PW only.

Comparisons between the estimation errors of each prediction method for all subjects were made using paired t-tests. Comparisons between subject groups (adults, children, and children with CP) for each method were made using unpaired t-tests (SPSS v.10.0, SPSS Inc. Chicago, IL. USA). The significance level was set at $p<0.05$.

The data collected from the MRI scans ($n = 32$) were also used to calculate new predictive equations of the form

$$\hat{x} = a(\text{PW}) + b(\text{PD}) + c(\text{LL}) + d, \quad (1)$$

where $\hat{x}$ is the predicted value of the HJC x coordinate, and a, b, c, and d are constants. The independent variables are pelvic width (PW), pelvic depth (PD, the distance between the midpoints of the line segments connecting the two ASIS and the two PSIS), and leg length (LL). Similar equations were written for the HJC coordinates y and z. PW and LL were included in the equations because they were used in the other methods tested; PD was added because it has been recommended

for use in the antero-posterior direction (Seidel et al., 1995). Although Seidel et al. (1995) also proposed using pelvic height to predict the supero-inferior HJC coordinate, this was not included since it relies on palpation of the pubic symphysis, a procedure not considered to be practical in routine clinical practice.

Two methods were used to assess which independent variables gave the best-fit regression model for the data: multiple linear regression and leave-one-out cross-validation (LOOCV). In a forward stepwise regression approach (Sokal and Rolf, 1995), the variable with the largest coefficient of determination (R^2), was the first entered into the model, provided the corresponding F statistic was significant at the $p<0.05$ level. The addition of further variables into the regression model was based on the increment in R^2 and its significance tested using a further F statistic.

LOOCV (Ripley, 1996) was used to give an indication of how well each regression equation would perform when predicting the HJC coordinates based on new input data for PW, PD, and LL. The existing data ($n=32$) was divided into two parts, a training set with $n-1$ data points and a test set with one data point. Using the training set, regression equations for each HJC coordinate $(\hat{x},\hat{y},\hat{z})$ were found and used to predict the HJC coordinates of the data in the test set. At this stage, the absolute error for each coordinate was recorded (for example, $|\hat{x}-x|$). The procedure was then repeated n times so that each data point in turn became the test set. The overall leave-one-out cross-validation errors (LOOCVE) were calculated as the mean of the absolute errors. All calculations for the regression equations were performed using Matlab (Mathworks, Inc., Natick, MA, USA).

3. Results

Subject details, PW, PD, LL, and the averaged coordinates for the left and right HJCs are listed in Table 1. The mean HJC asymmetry was 6.0 ± 3.3 mm. Inter- and intra-assessor repeatability for locating the HJC positions was less than 1.2 mm. Inter- and intra-assessor repeatability in identifying ASIS and PSIS coordinates was mostly within 2.5 mm (one slice width), but the maximum absolute difference between assessors was 4.4 mm and for the same assessor on different occasions was 3.6 mm. Inter- and intra-assessor repeatability of pelvic axis orientation was within 2.2°.

The magnitudes of the prediction errors were similar for Methods II and III (Fig. 2), with maximum resultant errors of 25 mm. The errors for Method I were slightly higher ($p=0.006$ compared to Method II, and $p=0.002$ compared to Method III), with a maximum resultant error of 31 mm. The resultant errors of the prediction methods (Fig. 2) were similar across the subject groups, except for a tendency for higher errors in adults compared with healthy children; this difference was only significant for Method III ($p=0.012$). The prediction errors for patients with cerebral palsy were slightly higher than those for healthy children, but this difference was not statistically significant.

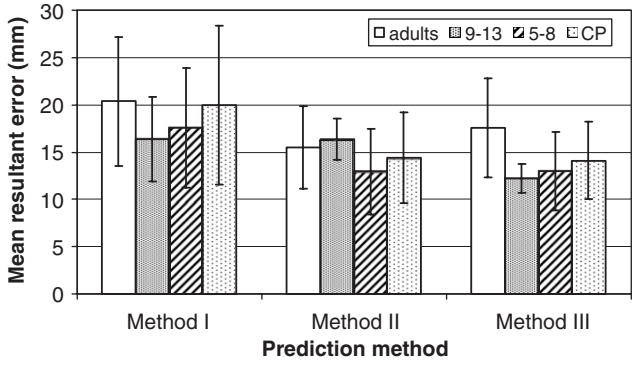

Fig. 2. Mean resultant errors in HJC location for the three tested prediction methods (Table 2) compared to the coordinates derived from the MRI images. The error bars indicate ± one standard deviation.

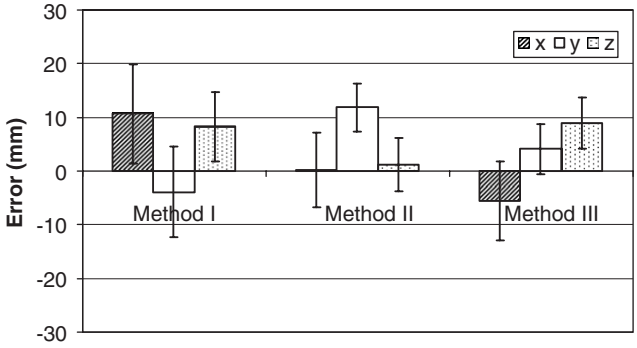

Fig. 3. Prediction errors in HJC location in the x, y, and z directions for all subjects for the three tested prediction methods (Table 2). 95% confidence intervals are shown.

When the mean prediction errors of each HJC coordinate were considered separately (Fig. 3), some were non-zero, indicating a bias. This was only significantly different from zero ($p<0.05$) for the y (supero-inferior) direction using Method II.

For single-variable regression, the best predictive variables according to R^2 and the F-statistic were PD for the x (antero-posterior) and z (medio-lateral) directions and PW and LL almost equally for the y (superior-inferior) direction (Table 3). For the x direction, there was no improvement in R^2 with the addition of further independent variables. A significant improvement in R^2 ($p<0.01$) was found in the y direction with the inclusion of both PW and LL, but the subsequent addition of PD was not significant. In the z direction, R^2 was significantly improved ($p<0.01$) when PW was included with PD; no further

Table 3
Multiple regression and LOOCV results for HJC location using different sets of predictive variables

Variables included	HJCx posterior–anterior			HJCy inferior–superior			HJCz medio-lateral		
	F stat	R^2	LOOCVE (mm)	F stat	R^2	LOOCVE (mm)	F stat	R^2	LOOCVE (mm)
PW			5.87			4.09			3.89
PD			5.39			5.50			4.41
LL			5.25			3.73			4.64
PW + Intcpt	17.33**	0.37	5.80	187.4**	0.86	3.76	188.8**	0.86	3.80
PD + Intcpt	29.29**	0.49	5.24	124.2**	0.81	4.57	216.8**	0.88	3.72
LL + Intcpt	23.55**	0.44	5.42	187.7**	0.86	3.76	143.1**	0.83	4.50
PD, PW + Intcpt	0.15 ns	0.50	5.38	5.70*	0.88	3.70	14.91**	0.92	3.22
PW, LL + Intcpt				9.16, 9.11**	0.90	3.58			
PD, LL + Intcpt	0.16 ns	0.50	5.36	3.52 ns		3.67	4.80*	0.90	3.55
PD, PW, LL + Intcpt				1.31 ns	0.90	3.64	0.05 ns	0.92	3.30

The "best-fit" single-variable regression F statistics and the lowest LOOCVEs are highlighted. ** indicates $p<0.01$, * indicates $p<0.05$, 'ns' indicates 'not signifcant' or $p>0.05$. R^2 values and F statistics are not presented for zero intecept regressions, since there is no direct comparison to those derived from models with constant terms. Note that the case "PW, LL + Intcpt" in the y-direction has two values for the F statistic, one for PW with LL added and one for LL with PW added.

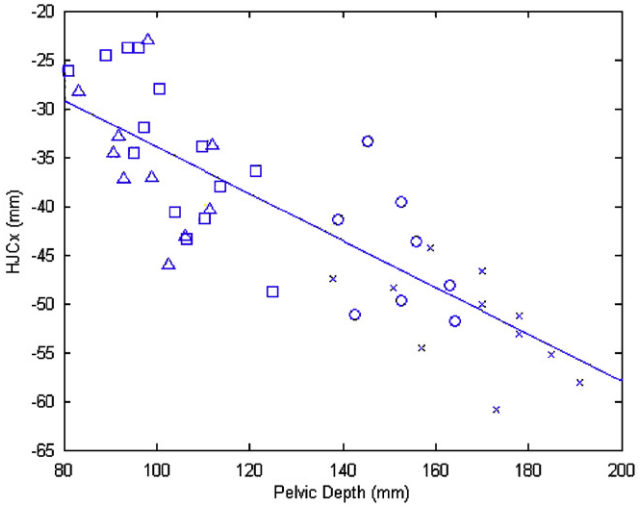

Fig. 4. Scatter plot of x coordinates of HJCs against PD, together with the regression line HJC$x = -0.24$PD $- 9.9$ derived from MRI scans (Table 1). ○ = healthy adults, □ = healthy children, △ = children with cerebral palsy. Coordinates taken from Leardini et al. (1999) (graphed as ×) are shown for comparison.

improvement was achieved by also including LL. The lowest LOOCVEs were consistent with the results from the stepwise regression. LOOCVEs were generally lower for single-variable regressions with intercepts compared to regressions through the origin.

Based on both stepwise regression and LOOCV, the resulting regression equations (in mm) for the right HJC are

$$\hat{x} = -0.24\text{PD} - 9.9, \quad (2)$$

$$\hat{y} = -0.16\text{PW} - 0.04\text{LL} - 7.1, \quad (3)$$

$$\hat{z} = 0.28\text{PD} + 0.16\text{PW} + 7.9. \quad (4)$$

Scatter-plots of HJC location from MRI against the predictive variables that maximised the F-statistic for single-variable regressions (open symbols in Figs. 4, 5a, 5b, and 6a) show an even spread of data for each subject group about the regression lines. For the data produced in this study, these plots support the choice of a linear regression rather than a higher order polynomial fit.

4. Discussion

This study used MRI for evaluating HJC prediction errors, whereas most previous studies (Bell et al., 1990; Leardini et al., 1999) used X-rays as the gold standard. MRI has the advantage of not exposing subjects to radiation, whilst still maintaining good accuracy. Repeatability of extracting HJC locations using sphere-fitting of points on the femoral head was found to be within 1.2 mm. In a previous MRI study in which similar techniques were used to identify anatomical landmarks (Jenkins et al., 2003), measurements of landmark separation were within 1.5 mm of those digitised from dissection. To achieve this level of accuracy, MRI scans need to be of good quality; differences between assessors of up to 4.4 mm were found for PSIS landmark identification when images were slightly blurred.

There can be significant error in predicting HJC location based on regression equations such as those used in commercial gait analysis packages. Resultant errors of up to 35 mm (Bell et al., 1990) and 22 mm (Seidel et al., 1995) and mean errors of 29 mm (Leardini

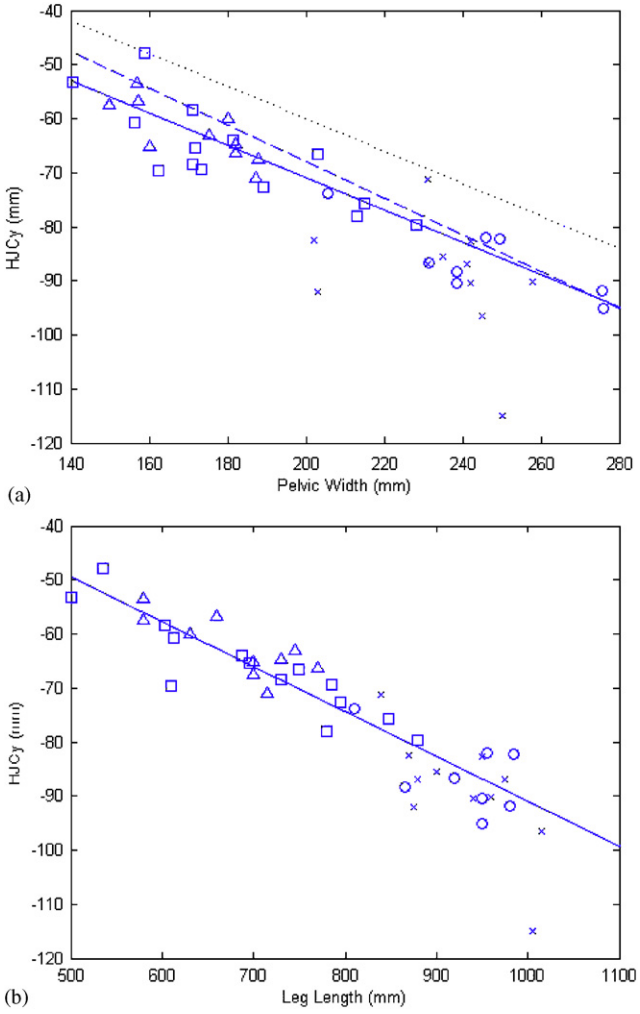

Fig. 5. (a) Scatter plot of y coordinates of HJCs against PW together with the regression line HJC$y = -0.30\text{PW} - 10.9$ derived from MRI scans (Table 1). (b) y coordinates of HJCs against LL together with the regression line HJC$y = -0.083\text{LL} - 7.9$ derived from MRI scans (Table 1). ○ = healthy adults, □ = healthy children, △ = children with cerebral palsy. Coordinates taken from Leardini et al. (1999) (graphed as ×) are shown for comparison. Dotted and dashed lines show in (a) are the prediction equations for Methods II and III, respectively.

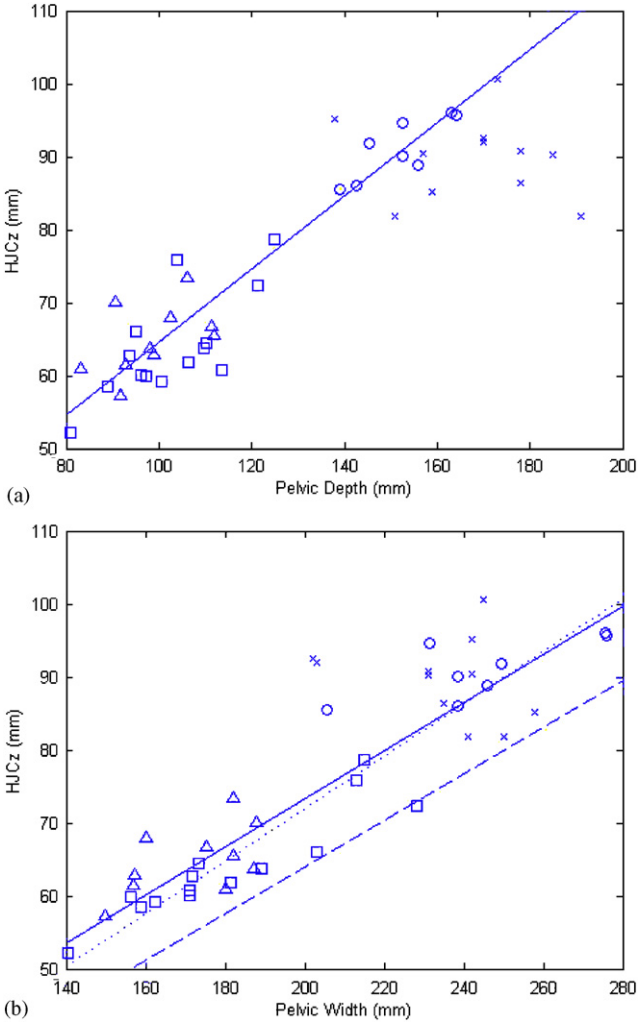

Fig. 6. (a) Scatter plot of z coordinates of right HJCs against PD together with the regression line HJC$z = 0.50\text{PD} + 14.7$ derived from MRI scans (Table 1). (b) z coordinates of right HJCs against PW together with the regression line HJC$z = 0.33\text{PW} + 7.3$ derived from MRI scans. ○ = healthy adults, □ = healthy children, △ = children with cerebral palsy. Coordinates taken from Leardini et al. (1999) (graphed as ×) are shown for comparison. Dotted and dashed lines show the prediction equations for Methods II and III, respectively.

et al., 1999) have been reported in adults. Since conventional regression equations have been based on average adult data, there has been concern that prediction errors would be greater in children and more-so in cerebral palsy (Fieser et al., 2000). Despite preliminary results that supported this theory (Jenkins et al., 2001), the results of the current study indicate that the errors in children are of a similar magnitude to those in adults. Furthermore, the errors in children with CP measured in this study are not significantly higher. The regression equations proposed by Bell et al. (1990) (Method II) and the ones recommended by OrthoTrak (Method III) gave results closest to those from MRI with maximum errors of 21 and 18 mm in children, compared with 26 mm using Method I, published by Davis et al. (1991). While these errors are comparable to those in adults, in relative terms they will be more significant in children, who have smaller pelvises. Accuracy could be further reduced during gait analysis by low inter-rater reliability in landmark palpation (Della Croce et al., 1999) and skin movement artefacts (Cappozzo et al., 1996).

Prediction errors of the magnitude reported in this study are likely to have only a small effect on resulting joint angles during gait (Stagni et al., 2000), but they could have a significant effect on joint kinetics. Stagni et al. (2000) showed that errors in the range of 30 mm in HJC in the anterior–posterior direction in adults caused

errors of 22% in the magnitude of hip flexion/extension moments and of 25% in their timing.

Asymmetries in HJC location of up to 13 mm (mean 6.0 mm) were found in this study; these arise from errors in data extraction and the inherent asymmetry in the subjects measured. These values are less than those reported by Leardini et al. (1999) of up to 25.9 mm (mean 12.6 mm). If true asymmetry in HJC location exists, this can never be accounted for by predictive equations that assume symmetry.

Regression analysis showed that it is reasonable to generalise HJC prediction equations across adults and children and the cerebral palsy patients in this study. For the x (antero-posterior) direction, pelvic depth (PD) was the best predictor of HJC. Although PD only explained 49% of the variation in x, the results are consistent with Seidel et al. (1995) who found PD to be the best predictor of HJC location in this direction in 65 adult human cadavers. The resulting regression equation is consistent with the coordinates reported by Leardini et al. (1999) based on a roentgen stereophotogrammetric study ($\times$ symbols in Fig. 4).

For the y (supero-inferior) direction, a combination of pelvic width (PW) and leg length (LL) was the best predictor of HJC. Although either variable alone can explain 86% of the variation in this direction, it could be argued that LL should not be included in the regression due to the low inter-rater reliability in its measurement. A single regression based on PW is plotted in Fig. 5a, along with the regression lines for Methods II and III. The results from Leardini et al.'s adult group (1999) ($\times$ symbols in Fig. 5a) tend to fall below all three regression lines. This difference is possibly related to methodological differences between the studies or may indicate differences in proportions for the adults in Leardini's study. Interestingly, the high correlation with PW in this direction contrasts with the results of Seidel et al. (1995) who found no correlation with PW. A single regression based on LL is plotted in Fig. 5b. Although the results from Leardini et al.'s adult group (1999) ($\times$ symbols in Fig. 5b) lie closer to the best-fit line than do those shown in Fig. 5a, the majority of points again lie below the regression line.

For the z (medio-lateral) direction, a combination of pelvic depth (PD) and pelvic width (PW) was the best predictor of HJC. Both these variables were highly correlated with the z direction, alone explaining 88% and 86% of the variation, respectively. When the resulting single regression equations (Figs. 6a and 6b) are compared with the coordinates reported by Leardini et al. (1999), the trend across both sets of results appears to be more consistent for the z direction if PW (Fig. 6b), rather than PD (Fig. 6a), is taken as the predictive variable, particularly for larger adults. This is consistent with the results of Seidel et al. (1995) who found a stronger correlation with PW than PD for this direction. Both Seidel et al. (1995) and Bell et al. (1990) found the HJC to be at 36% PW from the ASIS midpoint which is close to the results of the present study (dotted line in Fig. 6b).

Since the regression equations derived in this study have been based on the full dataset available, it is not possible to compare them directly to Methods I–III. However, results from the LOOCV give an indication of the power of the equations to predict new data. This is of the order of 5 mm in the x (antero-posterior) direction, and 4 mm in the z (infero-superior) and y (medio-lateral) directions, which compare favourably with errors from Methods I–III (mean directional errors of 4–12 mm).

In clinical use, any HJC prediction techniques must cope with a wider range of pathologies than those tested here. For instance, the CP subjects measured in this study did not suffer from significant hip dysplasia which is likely to cause higher prediction errors. Functional techniques of HJC location such as those first proposed by Cappozzo (1984) offer potential for improving accuracy (Leardini et al. 1999; Piazza et al., 2001; Schwartz and Rozumalski, 2005); however, these require subjects to perform specific range of motion trials which can be difficult to achieve with patients who may suffer from restricted hip motion and lack of stamina. Rozumalski and Schwartz (2004) have suggested a series of movements that are clinically acceptable including using facilitated passive movements when necessary. It remains to be seen how widely this will be adopted by clinical gait laboratories that are reluctant to add additional time to their gait assessments. A solution may be found in a combination of predictive and functional techniques. The new equations stated here could be applied and then optimised using the functional information inherent in gait data in a technique such as that proposed by Charlton et al. (2004).

5. Conclusion

The analysis of three popular predictive techniques for estimating HJC location showed that the prediction errors were similar across children and adults and a group of 10 young patients with spastic diplegic cerebral palsy. From a regression analysis, new predictive equations that generalise across these three groups were derived. Both stepwise linear regression and leave-one-out cross validation indicated the same combination of predictive variables for each HJC coordinate. These were pelvic depth (PD) for the x (antero-posterior) direction, pelvic width (PW) and leg length (LL) for the y (supero-inferior) direction and PD and PW for the z (medio-lateral direction). If comparisons with previous studies as well as practicalities and the reliability of measures in clinical practice are taken into account, the

following *single* linear regression equations (in mm) are proposed for the right hip:

$$\hat{x} = -0.24\text{PD} - 9.9, \quad (5)$$

$$\hat{y} = -0.30\text{PW} - 10.9, \quad (6)$$

$$\hat{z} = 0.33\text{PW} + 7.3. \quad (7)$$

Results in this study indicate that these could improve estimates based on existing predictive methods by up to 7 mm, depending on method and direction considered. However, predictive methods do not account for pelvic asymmetry, which was found to average 6 mm in this study, and do not account for errors in marker placement or skin movement artefacts.

Acknowledgements

The authors wish to acknowledge the financial support of The Wishbone Trust (UK), the Engineering and Physical Sciences Research Council (UK), and The Leverhulme Trust (UK); the clinical support from Mrs. Nicky Thompson, Oxford Gait Laboratory, and the Radiology Department of the Nuffield Orthopaedic Centre NHS Trust; and the helpful suggestions of Dr. Alberto Leardini.

References

Bell, A.L., Pedersen, D.R., Brand, R.A., 1990. A comparison of the accuracy of several hip center location prediction methods. Journal of Biomechanics 23 (6), 617–621.

Cappozzo, A., 1984. Gait analysis methodology. Human Movement Science 3, 27–50.

Cappozzo, A., Catani, F., Leardini, A., Benedetti, M.G., Della Croce, U., 1996. Position and orientation in space of bones during movement: experimental artifacts. Clinical Biomechanics 11 (2), 90–100.

Charlton, I.W., Tate, P., Roren, L., 2004. Repeatability of an optimised lower body model. Gait and Posture 20 (2), 213–221.

Davis, R.B., Õunpuu, S., Tyburski, D., Gage, J.R., 1991. A gait analysis data collection and reduction technique. Human Movement Science 10 (5), 575–587.

Della Croce, U., Cappozzo, A., Kerrigan, D.C., 1999. Pelvis and lower limb anatomical landmark calibration precision and its propagation to bone geometry and joint angles. Medical and Biological Engineering and Computing 37 (2), 155–161.

Fieser, L., Quigley, E.J., Wyatt, M., Sutherland, D., Chambers, H., 2000. Comparison of hip joint centers determined from surface anatomy and CT scans: two case studies. Gait and Posture 11 (2), 119–120.

Jenkins, S.E.M., Harrington, M.E., Theologis, T.N., Zavatsky, A.B., O'Connor, J.J., 2001. Errors in the calculation of the hip joint centre location in children. In: Proceedings of the XVIIIth Congress of the International Society of Biomechanics, p. 365.

Jenkins, S.E.M., Harrington, M.E., Zavatsky, A.B., O'Connor, J.J., Theologis, T.N., 2003. Femoral muscle attachment locations in children and adults, and their prediction from clinical measurement. Gait and Posture 18 (1), 13–22.

Kirkwood, R.N., Culham, E.G., Costigan, P., 1999. Radiographic and non-invasive determination of the hip joint center location: effect on hip joint moments. Clinical Biomechanics 14 (4), 227–235.

Leardini, A., Cappozzo, A., Catani, F., Toksvig-Larsen, S., Petitto, A., Sforza, V., Cassanelli, G., Giannini, S., 1999. Validation of a functional method for the estimation of hip joint centre location. Journal of Biomechanics 32 (1), 99–103.

Piazza, S.J., Okita, N., Cavanagh, P.R., 2001. Accuracy of the functional method of hip joint center location: effects of limited motion and varied implementation. Journal of Biomechanics 34 (7), 967–973.

Ripley, B., 1996. Pattern Recognition and Neural Networks. Cambridge University Press, Cambridge, UK.

Rozumalski, A., Schwartz, M.H., 2004. The practicality of functional model calibration in a clinical setting. In: Proceedings of the 13th Annual Meeting of the European Society for Movement Analysis in Adults and Children, p. 125.

Schwartz, M.H., Rozumalski, A., 2005. A new method for estimating joint parameters from motion data. Journal of Biomechanics 38, 107–116.

Seidel, G.K., Marchinda, D.M., Dijkers, M., Soutas-Little, R.W., 1995. Hip joint center location from palpable bony landmarks—a cadaver study. Journal of Biomechanics 28 (8), 995–998.

Sokal, R.R., Rolf, F.J., 1995. Biometry—the Principles and Practice of Statistics in Biological Research, third ed. W. H. Freeman and Co., New York.

Stagni, R., Leardini, A., Cappozzo, A., Benedetti, M.G., Cappello, A., 2000. Effects of hip joint centre mislocation on gait analysis results. Journal of Biomechanics 33 (11), 1479–1487.

Wu, G., 2002. ISB recommendation on definitions of joint coordinate system for various joints for the reporting of human joint motion. Part I: ankle, hip, and spine. Journal of Biomechanics 35, 543–548.